DTU Library

Actuator surface model for wind turbine flow computations

Shen, Wen Zhong; Sørensen, Jens Nørkær; Zhang, Jianhui

Published in:
Proceedings of European Wind Energy Conference 2007

Publication date:
2007

Document Version
Publisher's PDF, also known as Version of record

Actuator Surface Model for Wind Turbine Flow Computations

Wen Zhong Shen*[1], Jens Nørkær Sørensen[1] and Jian Hui Zhang[2]

[1]Department of Mechanical Engineering, Technical University of Denmark, Building 403, 2800 Lyngby, Denmark; *E-mail: shen@mek.dtu.dk; Phone: (45) 45 25 43 17; Fax: (45) 45 93 06 63.

[2]GE Energy, China.

Summary

The paper presents a new numerical technique for simulating wind turbine flows. The method, denoted as the actuator surface technique, consists of a three-dimensional Navier-Stokes solver and a body force distributed along the blade surfaces of a wind turbine. The force at each airfoil section is obtained from tabulated lift and drag coefficients, which depend on local angle of attack and resulting velocity. The local force is further distributed by a set of pre-determined functions that depends on angle of attack and airfoil shape. The pre-determined functions are curve-fitted using the TableCurve 2D software and based on pressure distributions obtained from a viscous-inviscid interactive code (XFOIL). The actuator surface technique is applied to compute the flow past a Nordtank 500kW turbine. Detailed comparisons with the previously developed Actuator Line model show that the new model determines more correctly the flow structures in the region close to the tips of the rotor blades.

1. INTRODUCATION

For predicting wind turbine performance, there exit many different methods. The most successful method is the classical Blade Element Momentum theory (BEM) which was first introduced by Glauert [1] to predict aerodynamic loading and power. In this model, the theory is based on one-dimensional momentum theory, with forces distributed continuously in the azimuth direction and tabulated two-dimensional airfoil data. The BEM technique is today a common industrial tool for predicting the structural dynamics and performance of wind turbines. The method is efficient and can be run on a personal computer. Although BEM is one-dimensional it is a rather reliable technique in the case of constant axial inflow, but it may degrade a lot in complex flow situations.

Since flows around wind turbines are essentially inviscid, vortex wake methods represent a suitable alternative for wind turbine predictions [2] [3] [4]. Using this technique, bound vortices are used to represent the lift in each airfoil section. In the wake of the rotor, trailing and shed vortices are used to describe the wake. The induced velocity at any position is computed using Biot-Savart's law, with contributions from bound and trailing vortices. Vortex methods can be divided into two types of models: prescribed wake models [2] and free wake models [3] [4]. The prescribed wake model gives fast results, whereas free wake models are more computing demanding and give more physical insight regarding the wake dynamics.

The third type of method is the Navier-Stokes based model (i.e., finite difference, finite volume or finite element methods) [5]-[10]. In the past ten years, computing power has been increased dramatically after the introduction of multiprocessor techniques with Message Passing Interface (MPI). Today it is possible to consider wind turbine flows as a whole by descretizing the three-dimensional Navier-Stokes equations using different numerical techniques. For a standard computation of the flow about a wind turbine, at least several millions of mesh points are needed and it takes a few days to get a solution. For general flow situations (general flow conditions and different turbine operations) the computing cost can increase considerably.

In order to cope with complex flow cases, we here propose to introduce body forces from tabulated airfoil data in a Navier-Stokes solver where a load is distributed on the rotor blades. The combined solver can provide a detailed flow solution from which angles of attack and relative velocities to airfoil sections can be determined.

Applying tabulated airfoil data gives the resulting force. There are two types of methods using this concept: the actuator disk models developed in [5]-[9] and the actuator line models in [10]. The actuator disk model distributes the loading continuously in azimuth direction and solves the axisymmetrical or three-dimensional Navier-Stokes equations. In order to improve the accuracy, the actuator disc model can be refined by replacing it with a so-called actuator line, introduced by Sørensen and Shen [10]. The model solves the three-dimensional Navier-Stokes equations with an aerodynamic loading distributed along lines representing blade forces. The technique gives a more physical representation of the wind turbine blades. It can be used to simulate flow around wind turbines in complex situations. However, if we focus on the flow in a cross section of blade, the actuator line contains only one point to represent an airfoil. From two-dimensional modeling, it is difficult to represent the flow past an airfoil or a solid body using one point force plus a uniform flow and it is thus needed to develop a model that can represent the real flow past an airfoil. Thus a 2D Actuator surface model has been developed [11] [12]. In order to simulate wind turbine flow, the model needs to be extended to three dimensional flows. The goal of the present paper is to develop a three-dimensional actuator surface model.

The paper is organized as follow. In section 2, the methodology of the three-dimensional actuator surface model is described. In section 3, the force distribution along an airfoil chord is summarized. In section 4, the 3D actuator surface model is applied for flows past a Nordtank 500 kW wind turbine at a wind speed of 10 m/s and compared to the previous developed actuator line model.

2. THREE-DIMENSIONAL ACTUATOR SURFACE MODEL

2.1 Navier-Stokes solver

The three-dimensional Navier-Stokes solver used here is the EllipSys3D code developed at Technical University of Denmark [13] in collaboration with Risø National Laboratory [14]. The code is based on a finite-volume method with multi-block strategy. It allows to be run in parallel computers with Message Passing Interface (MPI). The governing equations consist of three components of the momentum equation and the continuity equation:

$$\rho\left(\frac{\partial \vec{u}}{\partial t} + (\vec{u}\cdot\nabla)\vec{u}\right) = -\nabla p + \mu\nabla^2\vec{u} + \vec{f}_b \tag{1}$$

$$\nabla\cdot\vec{u} = 0 \tag{2}$$

where $\vec{u}$ denotes the velocity vector, ρ is the density, *p* is the pressure, μ is the viscosity and $\vec{f}_b$ is the body force. The equations are solved by a predictor-corrector method combined with the improved Rhie-Chow interpolation scheme developed in [15]. The pressure Poisson equation is solved by using a 5-level multi-grid technique.

2.2 Determination of body force

The body force at each cross section is found using tabulated 2D airfoil data that are corrected for 3D rotational effects:

$$\vec{f}_{2D} = \frac{1}{2}\rho V_{rel}^2 c(C_L\vec{e}_L + C_D\vec{e}_D)F_{dist} \tag{3}$$

where (C_L, C_D) are the lift and drag coefficients, *c* is the airfoil chord, F_{dist} is the distribution of pressure force along the airfoil chord that will be discussed in section 3.2 and $\vec{V}_{rel}$ is the relative velocity at a control point located in the rotor plan of the airfoil cross section, see figure 1:

$$\vec{V}_{rel} = (u_c - u_{in}, v_c - v_{in}) \tag{4}$$

where $\vec{u}_c = (u_c, v_c)$ is the local velocity and $\vec{u}_{in} = (u_{in}, v_{in})$ is the induced velocity at the control point contributed only from bound circulations along blades. The methodology of the Actuator Surface model is shown in Fig. 1. From the figure, it is seen that the actuator surface model is consisted of a series of 2D actuator surface models that are applied in each cross section of the rotor blades where a force is distributed along the airfoil chord to represent the airfoil section.

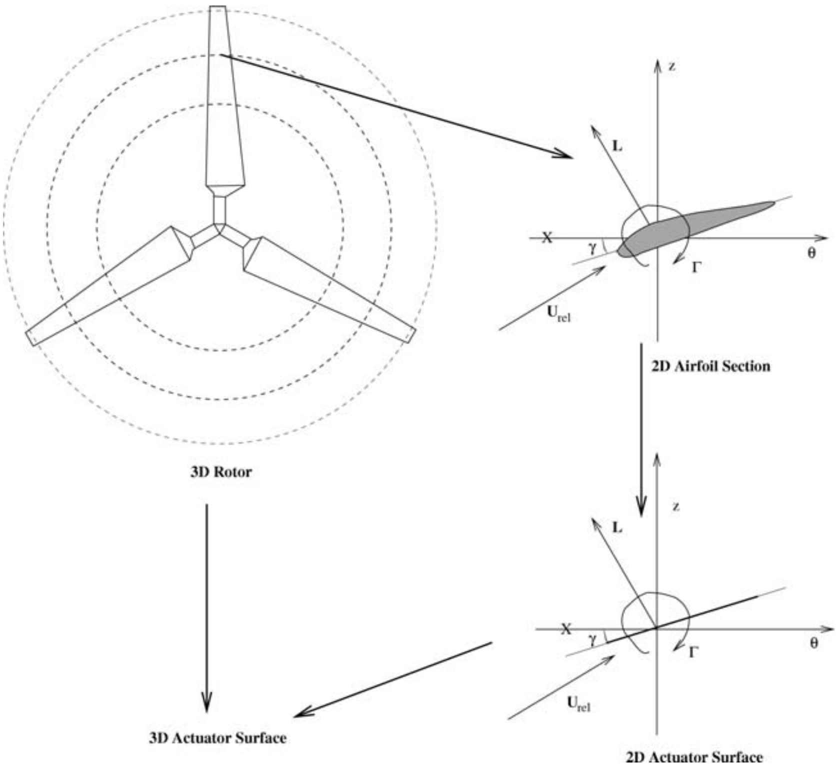

Figure 1: Geometry configuration of a wind turbine where x represents the location of a control point and Γ is the circulation.

The induction can be computed by using Biot-Savart's law:

$$\vec{u}_{in}(\vec{x}) = \frac{1}{4\pi}\sum_{i=1}^{nb}\int_0^R\int_{y_l}^{y_t}\frac{\Gamma_i(y,r)\vec{e}_r \times (\vec{x} - \vec{y}(y,r))}{|\vec{x} - \vec{y}(y,r)|^2}dydr \tag{5}$$

where *nb* is number of blades and y represent chord wise integration from the leading edge y_l to the trailing edge y_t of the airfoil section. In order to determine the relationship between bound circulation and airfoil lift, the Kutta-Joukowshi law is used as a first order approach:

$$L_i(y,r)\vec{e}_L = \rho\vec{V}_{rel}(r) \times \Gamma_i(y,r)\vec{e}_r \tag{6}$$

When the relative velocity is known, flow angle ϕ and angle of attack α are determined from

$$\phi = \tan^{-1}\frac{v_c - v_{in}}{u_c - u_{in}}$$
$$\alpha = \phi - \beta - \gamma \tag{7}$$

where β is pitch angle and γ is twist angle.

Since the force is only acting on the rotor blades, it may cause sharp changes in the area near the leading edge lines. This may result in difficulties for the flow solver to achieve stable solutions and numerical wiggles may arise. In order to overcome the difficulty, a regularization function is applied on the body force $\vec{f}$:

$$\vec{f}_b(\vec{x}) = \vec{f}_{2D} \otimes \eta_\varepsilon = \sum_{i=1}^{nb} \int_0^R \int_{y_l}^{y_t} \vec{f}_{2D}(y,r) \cdot \eta_\varepsilon \left(\left| \vec{x} - \vec{y}(y,r) \right| \right) dy dr \tag{8}$$

where the kernel of regularization is the Gaussian distribution

$$\eta_\varepsilon(r) = \frac{1}{\varepsilon^3 \pi^{3/2}} \exp\left[- \left(r/\varepsilon \right)^2 \right] \tag{9}$$

3. DETERMINATION OF FORCE DISTRIBUTIONS ON AIRFOIL SECTIONS

3.1 Tabulating data

In order to parametrically study force distributions around airfoil sections, the viscous-inviscid interaction code XFOIL [16] has been used. The code solves the boundary layer equations in the viscous boundary layer close to airfoil and wake and Euler equations in the inviscid zone outside of the viscous domain. The code can easily to run on a personal computer and is therefore suitable for studying the dependency of force distributions on different parameters, such as the airfoil shape, Reynolds number and angle of attack. The XFOIL code has been validated against other numerical methods and experimental data (for example, at low and moderate angles of attack [17] [18] and at high angles of attack [11]). Since the force distribution along the airfoil chord is mainly due to the difference of pressure forces on the pressure side and the suction side, it is convenient to consider only the pressure difference. For more information, the reader is referred to [11].

3.2 Empirical formulae of force distributions

In order to get a general empirical relation for force distributions, we need to perform a parametrical study of pressure coefficients on flows past airfoils under various conditions. When the data are achieved, the software TableCurve 2D [19] is used for deriving empirical formulae. The empirical formulae should be able to take into account all influences from all relevent parameters, such as airfoil thickness, airfoil chamber, Reynolds number and angle of attack. Using the meshing curve in TableCurve 2D, the following two basic functions are obtained:

$$f(x) = \left[A + B \exp\left(- \frac{\ln 2 \ln^2 \left(1 + (x - C)(E^2 - 1)/(DE) \right)}{\ln^2 E} \right) \right] f_T \tag{10}$$

$$f(x) = \left[\frac{A + Cx^{0.5} + Ex + Gx^{1.5}}{1 + Bx^{0.5} + Dx + Fx^{1.5}} \right] f_T \tag{11}$$

where the coefficients A, B, C, D, E, F and G are functions of angles of attack and f_T is a function of airfoil thickness. For more details, the reader is referred to [11].

4. RESULTS AND DISCUSSIONS

The actuator surface model is applied to flow past a Nordtank 500kW wind turbine equipped with three LM 19.1 blades. In figure 2, the surface consisting of chord lines where the load is distributed is plotted.

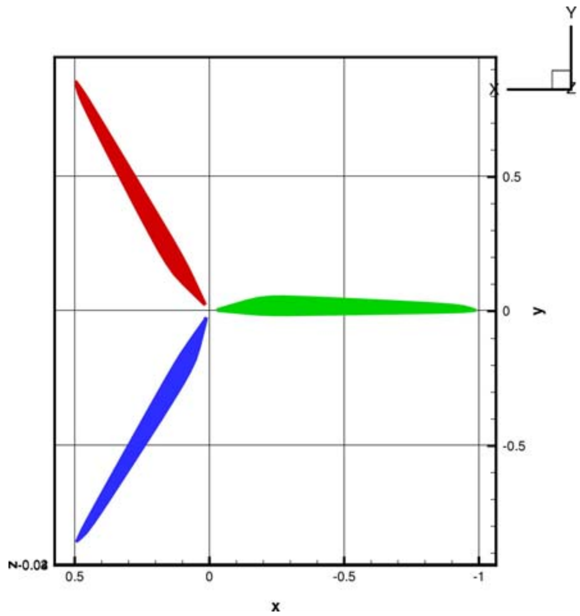

Figure 2: Blade surface where force is applied on.

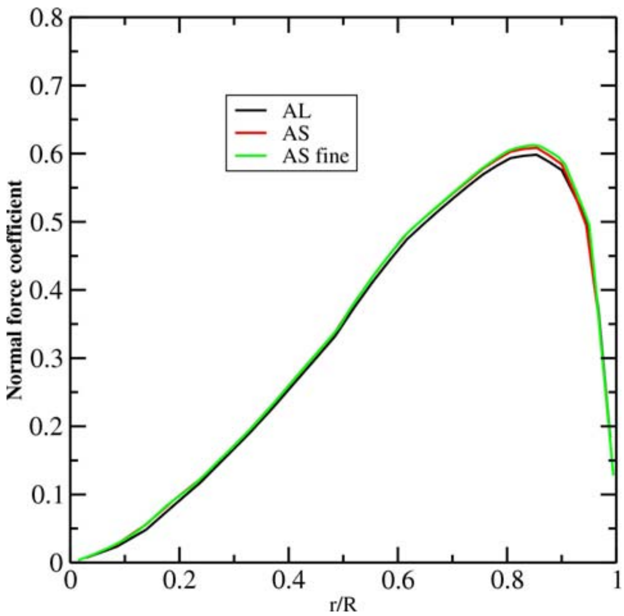

Figure 3: Normal force coefficient along the blade at a wind speed of 10 m/s.

To limit the computational domain, only one of the three blades is taken into account in the computations mesh where periodic boundary conditions are used in the azimuth direction. The computational domain covers a volume corresponding to $[0,8.5R]\times[0,2\pi/3]\times[-12.8R,19.5R]$ in radial, azimuth and axial directions, respectively where R is the rotor radius. The computational domain is then divided into 4 blocks of 48x48x48 mesh points. In order to have a fine resolution near the blade tip, the mesh is stretched in axial and radial directions. The rotor is placed at z=0 and the blade radius is discretized by 30 computational mesh points. In order to solve the problem more accurately, a finer mesh consisting of 9 blocks of 64x64x64 mesh points stretched towards the rotor blade is also used. In the fine mesh, the number of mesh points is doubled on the blade (60 points) and in the tangential direction it is stretched in order to obtain an almost cubic mesh near the blade tip.

Actuator Surface computations were carried out for a Nordtank 500 kW turbine at a wind speed of 10 m/s. In order to validate the model, the obtained results are compared with those of the Actuator Line model [9]. The normal force coefficient is plotted in Fig. 3. From the figure, it is seen that the Actuator Surface predicts almost the same results as the actuator line model and grid refinement does not influence the force curve. The axial velocity in the *r-z* plan where the blade is located is plotted in Fig. 4. From the figure, it is seen that the axial velocity maintains the form but the field obtained from the Actuator surface model contains more information near the tip and in the tip vortex region. In Fig. 5, the axial interference factor is plotted. From the figure, it is seen that the interference factor predicted by the actuator surface model is slightly smaller than that by the actuator line model. Moreover, the value of the interference factor at the tip predicted by the AS model is small but not exactly zero. A similar behaviour has been observed in the data extracted from RANS computations of the Tellus 95 kW turbine [20] (see Fig. 6).

(a) (b) (c)

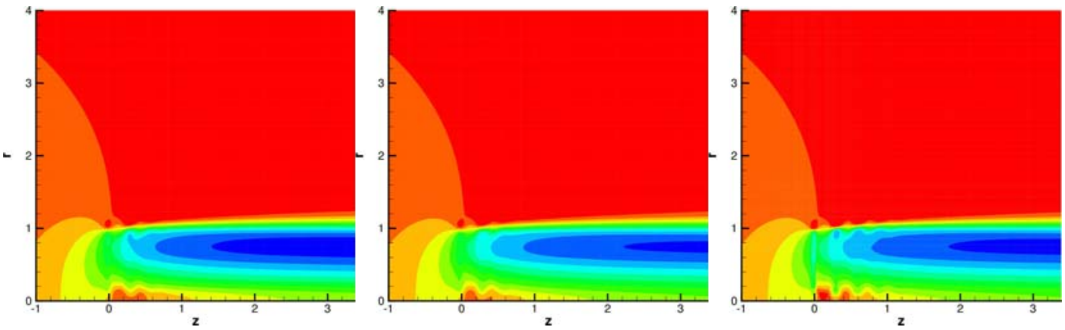

Figure 4: Axial velocity plot in the r-z plan; (a) Actuator line model; (b) Actuator Surface model; (c) Actuator Surface model with the fine mesh.

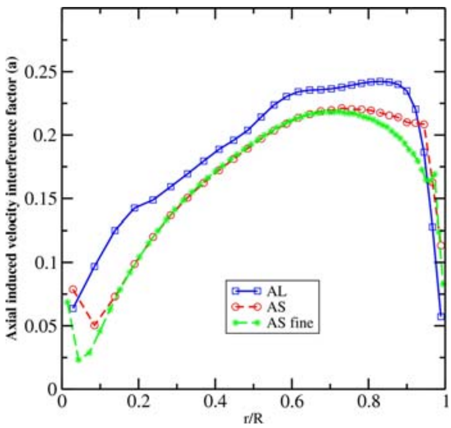

Figure 5: Axial induced velocity interference factor for Nordtank 500 kW at a wind speed of 10 m/s.

In order to visualize the flow structures near the blade, we focus on the flow in the cross section r=0.6R. In Fig. 7, the streamlines are plotted. From the figure, it is seen that the streamlines cross the airfoil chord in (a) and (b) but it passes the airfoil smoothly in case (c). The difference between cases (b) and (c) is that only 3 mesh points are used to describe the airfoil chord in (b) whereas 8 points are used in (c). This shows that a fine mesh would be needed in order to predict correctly the flow structure. The thrust and power coefficients are summarized in Table 1. From the table, it is seen that the difference is less than a few percent.

Table 1: Thrust and power coefficients for a Nordtank 500 kW at a wind speed of 10 m/s.

Model	Mesh	Ct	Cp
AL	96x48x96	0.599	0.415
AS	96x48x96	0.579	0.407
AS Fine	192x64x192	0.586	0.414

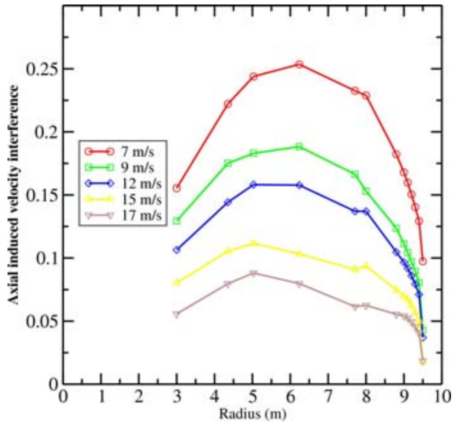

Figure 6: Axial induced velocity interference factor for Tellus 95 kW (data extracted from RANS computations [20]).

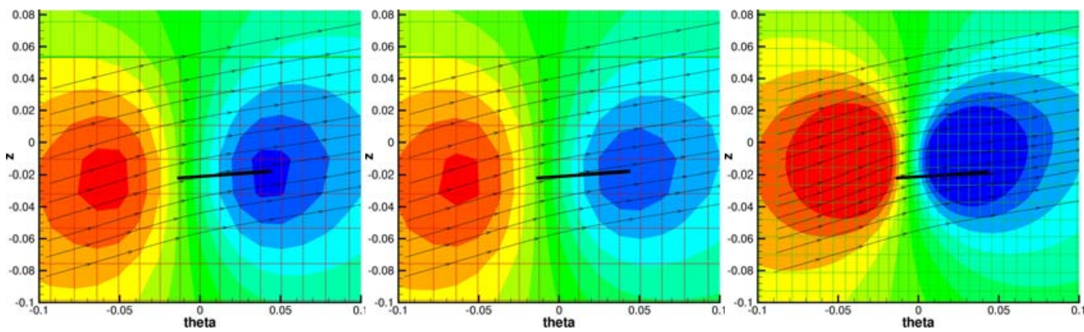

Figure 7: Stream line and axial velocity plot in the cross section (r=0.65R); (a) Actuator line model; (b) Actuator Surface model; (c) Actuator Surface model with the fine mesh.

5. CONCLUSION

The actuator surface technique is combined with the incompressible Navier-Stokes equations and applied to a Nordtank 500 kW wind turbine at wind speed of 10 m/s. The loading is both distributed along the span of the rotor blades and along the airfoil chord in each cross section. Computations show that the Actuator Surface technique more correctly predicts the flow structure near blades and in the tip vortex region. At the rotor blade, the flow predicted by the Actuator surface model on a finer mesh passes smoothly the airfoil.

The Nordtank turbine uses 3 LM 19.1 blades with very small airfoil chords in the outer part of the blade. Modern turbines have relatively big airfoil chords in the tip region before the blade ends. The new model needs to account such situations.

References

1. Glauert, H., Airplane propellers. In Aerodynamic theory, (Ed. W.F. Durant), Dover Publication Inc.: New York, 1963, Vol. 4, Division L, 169-360.
2. Wilson, R.E., Lissaman, P.B.S. and Walker, S.N., Aerodynamic performance of wind turbines, Oregon State University, 1976.
3. Strickland, J.H., Webster, B.T. and Nguyen, T., A vortex model of the Darrieus turbine: an analytical and experimental study. Journal of Fluids Engineering, 1979, Vol. 101, 500-505.
4. Bareiβ, R. and Wagner, S., The free wake/hybrid wake code ROVLM – A tool for aerodynamic analysis of wind turbines. Proc. of the European Wind Turbine Conference, 1993, 424-431.
5. Sørensen, J.N. and Myken, A., Unsteady actuator disc model for horizontal axis wind turbines. Journal of Wind Engineering and Industrial Aerodynamics, 1992, Vol. 39, 139-149.
6. Sørensen JN, Shen WZ, Munduate X., Analysis of wake-states by a full-field actuator disc model. Wind Energy, 1998, Vol. 1, 73-88.
7. Mikkelsen, R., Sørensen, J.N. and Shen, W.Z., Modelling and analysis of the flow field around a coned rotor. Wind Energy, 2001, Vol. 4, 121-135.
8. Masson, C., Smaili, A. and Leclerc, C., Aerodynamic analysis of HAWTs operating in unsteady conditions. Wind Energy, 2001, Vol. 4, 1-22.
9. Sørensen, J.N. and Shen, W.Z., Numerical modeling of wind turbine wakes. Journal of Fluids Engineering, ASME Trans., June 2002, Vol. 124, 393-399.
10. Shen, W. Z., Sørensen, J.N. and Mikkelsen, R., Tip loss correction for Actatutor / Navier-Stokes computations. Journal of Solar Energy Engineering, 2005, Vol. 127, 209-213.
11. Zhang, J.H., Numerical modeling of vertical axis wind turbine (VAWT). Technical University of Denmark, 2004, MEK-FM-EP 2004-11, Denmark.
12. Shen, W.Z., Zhang, J.H., Sørensen, J.N. and Mikkelsen, R., Numerical modeling of vertical axis wind turbine flows using 2D Actuator Surface technique. In preparation.
13. Michelsen, J. A., “Basis3D-A platform for development of multi-block PDE solvers”, Technical University of Denmark, 1992, AFM 92-05, Lyngby, Denmark.
14. Sørensen, N. N., “General purpose flow solver applied over hills”, Risø National Laboratory, 1995, RISØ-R-827-(EN), Roskilde, Denmark.
15. Shen, W.Z., Michelsen, J.A., and Sørensen, J.N., Improved Rhie-Chow interpolation for unsteady flow computations. AIAA Journal, 2001, Vol. 39, No. 12, 2406-2409.
16. Drela, M.: XFOIL: An analysis and design system for low Reynolds number airfoils. Conference on Low Reynolds Number Aerodynamics. University of Notre Dame, 1989.
17. Fuglsang, P., Antoniou, I., Sørensen, N. and Madsen, H.A., Validation of a wind tunnel testing facility for blade surface pressure measurements 1998, Risø National Laboratory, Risø-R-981(EN), Denmark.
18. Fuglsang, P., Antoniou, I., Bak, C. and Madsen, H.A., Wind tunnel test of the Riso-1 airfoil. 1998, Risø National Laboratory, Risø-R-999(EN), Denmark.
19. http://www.sciencedownload.com/Graph_Plotting/Curve_Fitting/TableCurve_2D/.
20. Hansen M.O.L .and Johansen J., Tip studies using CFD and comparison with tip loss models, Wind Energy, 2004, Vol. 7, pp. 343-356.